# Changes in significant and maximum wave heights in the Norwegian Sea

Xiangbo Feng[1,2*], M. N. Tsimplis[1], M. J. Yelland[1] and G. D. Quartly[3]

[1] National Oceanography Centre, Southampton, UK

[2] School of Ocean and Earth Science, University of Southampton, UK

[3] Plymouth Marine Laboratory, Plymouth, UK

*Corresponding author address: National Oceanography Centre, Southampton, European Way, Southampton SO14 3ZH, UK

Email: xiangbo.feng@soton.ac.uk

## Abstract

This paper analyses 10 years of in-situ measurements of significant wave height ($H_s$) and maximum wave height ($H_{max}$) from the ocean weather ship *Polarfront* in the Norwegian Sea. The 30-minute ship-borne wave recorder measurements of $H_{max}$ and $H_s$ are shown to be consistent with theoretical wave distributions. The linear regression between $H_{max}$ and $H_s$ has a slope of 1.53. Neither $H_s$ nor $H_{max}$ show a significant trend in the period 2000-2009. These data are combined with earlier observations. The long-term trend over the period 1980-2009 in annual $H_s$ is 2.72±0.88 cm/year. Mean $H_s$ and $H_{max}$ are both correlated with the North Atlantic Oscillation (NAO) index during winter. The correlation with the NAO index is highest for the more frequently encountered (75th percentile) wave heights. The wave field variability associated with the NAO index is reconstructed using a 500-year NAO index record. $H_s$ and $H_{max}$ are found to vary by up to 1.42 m and 3.10 m respectively over the 500-year period. Trends in all 30-year segments of the reconstructed wave field are lower than the trend in the observations during 1980-2009. The NAO index does not change significantly in 21st century projections from CMIP5 climate models under scenario RCP85, and thus no NAO-related changes are expected in the mean and extreme wave fields of the Norwegian Sea.

**Keywords**: significant wave height; maximum wave height; Ship-Borne Wave Recorder; NAO; Norwegian Sea

## 1. Introduction

Large ocean waves pose significant risks to ships and offshore structures. The development of offshore installations for oil and gas extraction and for renewable energy exploitation requires knowledge of the wave fields and any potential changes in them. Most information presently available for wave fields is presented in terms of the significant wave height ($H_s$), which is defined as the average height of the highest one-third of the waves or, alternatively, as four times the square root of the zeroth moment of the wave spectrum (*Sverdrup and Munk*, 1947; *Phillips*, 1977). Knowledge of the maximum peak-to-trough wave height ($H_{max}$) is not usually available although these largest waves have the greatest impact on ships and offshore structures.

The *OWS Polarfront*, the last weather ship in the world, made measurements of $H_s$ for 30 years using a Ship-Borne Wave Recorder (SBWR). The ship was located at Ocean Weather Station Mike (OWS Mike, 66°N, 2°E, see Figure 1) in the Norwegian Sea. Waves observed using SBWRs at other stations have been systematically validated against wave buoys in terms of $H_s$ and spectrum by *Graham et al* (1978), *Crisp* (1987) and *Pitt* (1991). However in this study we also use $H_{max}$ from the SBWR which has not previously been validated against other wave measuring devices. By analysing the statistical relationship between $H_s$ and $H_{max}$ as measured by the SBWR and comparing it with the known theoretical and empirical relationships we indirectly provide confidence for the validity of the $H_{max}$ measurements.

The wind field over the North Atlantic is related to the North Atlantic Oscillation (NAO), a major large-scale atmospheric pattern in this region (*Hurrell*, 1995;

*Hurrell and Van Loon*, 1997; *Osborn et al.*, 1999). The status of the NAO is represented by the NAO index, determined from the non-dimensional sea level pressure difference between the Icelandic Low and the Azores High. The NAO is particularly important in winter, and *Bacon and Carter* (1993) were the first to note the link between this large weather pattern and the wave climate over the North Atlantic. An increase in $H_s$ in the North Atlantic over the second half of the $20^{th}$ century was found be associated with the NAO index variability (*Bacon and Carter*, 1993; *Kushnir et al*., 1997; *Wang and Swail,* 2001, 2002; *Woolf et al.,* 2002; *Wolf and Woolf*, 2006). In addition, linear regressions between the inter-annual $H_s$ anomalies and the NAO index have been established for various methods of wave height estimation (e.g. in-situ measurements, visual observations, satellite altimetry and numerical models) (*Bacon and Carter*, 1993; *Gulev and Hasse*, 1999; *Woolf et al*., 2002; *Wang et al*., 2004; *Tsimplis et al*., 2005). Hindcasts from numerical models suggest that the influence of the NAO extends to the largest 1% of $H_s$ in the North Atlantic during winter (*Wang and Swail,* 2001, 2002). *Izaguirre et al.* (2010) using satellite $H_s$ data also indicated that along the Atlantic coast of the Iberian peninsula the extreme wave climate is significantly associated with the NAO.

Thus there is a well-established relationship between $H_s$ and the NAO index during winter. The two terms, $H_{max}$ and $H_s$ are both characteristics of the wave field and both increase with increasing winds or increasing durations of a consistent wind. $H_s$ is governed by the mean conditions; however $H_{max}$ is not fully determined by the mean conditions but is also affected by local conditions as well as randomness. $H_{max}$ is the pertinent parameter for describing risks associated with operation of ships or offshore structures, hence it is important that we analyze both these measures of the wave field in a consistent manner to show how they differ.

In this paper, we investigate $H_s$ and $H_{max}$ using 10 years of 30-minute surface elevation records from the SBWR at OWS Mike in the Norwegian Sea. First we assess the validity of the dataset by comparing the observational distributions of $H_{max}$ and the $H_{max}/H_s$ ratio with the corresponding theoretical distributions. We establish that the $H_s$ and $H_{max}$ data obtained from the SBWR behave as expected on the basis of theoretical distributions that have been tested against other wave measuring systems. Thus this provides evidence that the $H_{max}$ from the SBWR are reliable. We then explore the relationships of the inter-annual changes in $H_s$ and $H_{max}$ with the NAO index. We also use a 500-year NAO index record to reconstruct the range of values that $H_s$ and $H_{max}$ may have had over the same period.

The paper is structured as follows. The data processing and methodology are described in Section 2, along with the statistical definitions to be used. In this section a comparison of the expected distributions for $H_s$ and $H_{max}$ with the observed distributions is made. In Section 3, the temporal variability of $H_s$ and $H_{max}$ are described, and is correlated with the winter NAO index. The results are discussed in Section 4 where also the natural variability of the wave field over the past 5 centuries is estimated from a reconstruction of the NAO index. Outputs from the most recent CMIP5 models are also used to infer changes in the NAO index under climate change scenarios, and hence assess the likely overall change of the wave fields in the 21st century. Our conclusions are given in Section 5.

## 2. Data and methodology

### 2.1. Ship-Borne Wave Recorder (SBWR) data

Ocean Weather Station Mike (OWS Mike, 66°N, 2°E, with 2000 m water depth) was occupied by weather ships for more than 60 years until the ship *Polarfront* was withdrawn at the end of 2009. Sea surface elevation has been measured by a Ship-Borne Wave Recorder (SBWR) and wave height data from this system are available from 1980 to the end of 2009.

The SBWR was developed by the UK National Institute of Oceanography (later to become part of the National Oceanography Centre) in the 1950s and is considered a very reliable system (*Graham et al*., 1978; *Holliday, et al*., 2006). The principles of operation of the SBWR are described in detail by *Tucker and Pitt* (2001). Using 13 years of data from three different weather ships stationed on the UK continental shelf, *Graham et al* (1978) demonstrated that $H_s$ values from the SBWR were 8% larger than those from WaveRider buoys on average, with closer agreement at larger wave heights. *Crisp* (1987) examined the wave spectra, and found that the frequency response of the SBWR differed from that of the WaveRider. *Pitt* (1991) developed an empirical frequency-response correction for the SBWR and this reduced the overestimation of $H_s$ to 5%. A short, 30-hour comparison between observations obtained on *Polarfront* and those from a WaveRider buoy also found good agreement, but in this case the SBWR underestimated the $H_s$ slightly, by 0.4 m on average (*Clayson*, 1997). Hence $H_s$ data from the SBWR are well validated.

From 1980 until the end of 1999, only the integrated wave parameters (e.g. $H_s$ and average period) were recorded by the SBWR system on *Polarfront*: these have been analysed briefly elsewhere (*Yelland et al*., 2009). However, for the last 10 years of operation (2000-2009, the period investigated in this paper) the SBWR system also recorded the sea surface elevation every 0.59 s for the 30-minute sampling periods, with sampling occurring once every 90 minutes before the 250$^{th}$ day of 2004, and once every 45 minutes thereafter. Tests made by sub-sampling data in the latter period to replicate the earlier 90-minute observational interval showed that the change in the observation interval in 2004 has no impact on the results discussed in the rest of this paper.

*Polarfront* was allowed to drift freely within a 32 km radius around OWS Mike. Once outside this radius the ship returned on station with a speed of up to 5 m/s. Some of the 30-minute records obtained while the ship was steaming were found to contain unrealistically large elevations. All spurious elevations when the ship was steaming were excluded from the analysis during quality control. The wave data during the periods when the *Polarfront* returned to port, 3 days out of every 28-day period, were omitted because the ship was not on station. A summary of the data record, after application of quality control, is provided in Figure 2.

The height of an individual wave is defined as the vertical distance between a wave trough and the following wave crest. There are 17,389,559 individual waves in a total of 71,210 thirty-minute wave records obtained over 2,915 days between 2000 and 2009. For each 30-minute record, the highest individual wave is identified as $H_{max}$, and $H_s$ is calculated from four times the square root of the zeroth-order moment of the wave frequency spectrum.

## 2.2. Statistical distribution of waves

This section briefly describes statistical distributions in theories for wave fields which have been verified against data obtained from bottom-mounted sensors, buoys and altimeters (*Bretschneider*, 1959; *Dobson et al.*, 1987; *Sterl et al.*, 1998; Tucker *and Pitt,* 2001; *Stansell*, 2004; *Vandeve*r *e*t *al.*, 2008; *Casas-Prat and Holthuijsen*, 2010). These statistical distributions are then used to validate the SBWR measurements of $H_{max}$ and other extreme wave conditions from the *Polarfront*. This is needed because, unlike $H_s$, $H_{max}$ data from the SWBR have not been validated previously.

Individual wave heights with a narrow-band spectrum are found to follow a Rayleigh distribution in the deep sea (*Longuet-Higgins*, 1952). Within this narrow-band spectrum of wave heights, the average height of the highest one-third of the waves over an observational period, $H_{1/3}$, is practically equal to the significant wave height, $H_s$, that can be derived from the spectrum (*Phillips,* 1977). The ratio of observed maximum wave height $H_{max}$ to $H_s$ can be theoretically presented as a function of $N$, the number of individual crest-to-trough waves measured during an observational period (*Sarpkaya and Isaacson*, 1981):

$$\frac{H_{\max}}{H_s} = \frac{\sqrt{\ln N}}{1.42} \tag{1}$$

Thus, if $N$ and $H_s$ are known, the probable maximum wave height $H^*_{\max}$ in a given period can be calculated using Eq. (1).

However, Eq. (1) has been found to overestimate the largest individual wave heights when compared to observations (*Forristall*, 1978; *Tayfun*, 1981; *Krogstad*, 1985; *Massel*, 1996; *Nerzic and Prevosto*, 1997; *Mori et al*., 2002; *Casas-Prat and Holthuijsen*, 2010). Some of the discrepancy has been attributed to the effect of the spectral bandwidth, i.e. the gathering of wave components around the peak energy component (*Tayfu*n, 1981; *Och*i, 1998; *Vandeve*r *e*t *a*l., 2008). When the spectral bandwidth increases, $H_s$ is overestimated compared with $H_{1/3}$ (*Tayfu*n, 1981; *Och*i, 1998; *Vandever et al*., 2008). This, in turn, will result in an overestimation of $H^{*}_{\max}$ estimated from Eq. (1). The nonlinearity of wave-wave interaction has also been found to affect the crest height and trough depth distributions, but not the peak-to-trough wave height distributions in observations [*Tayfu*n, 1983; *Casas-Prat and Holthuijsen*, 2010]. More recent laboratory and theoretical work has suggested that nonlinearity may also have some effect on wave height distribution, depending upon the state of wave development (*Sluryaev and Sergeeva*, 2012; *Ying and Kaplan*, 2012).

*Forristall* (1978) and *Gemmrich and Garrett* (2011) have shown that the Weibull distribution provides a better estimate of the observed largest wave heights, i.e. those with the lowest probability of occurrence. *Forristall* (1978) suggested that a correction to the $H_{max}$ derived from the Rayleigh distribution based on the number of waves in the observational record improves the agreement with the $H_{max}$ estimated from the Weibull distribution. This is supported by the results of *Casas-Prat and Holthuijsen* (2010). Thus the corrected Rayleigh distribution is an adequate approximation of the wave field parameters as measured by various wave-measuring platforms. In the absence of direct evaluation of $H_{max}$ from the SBWR against another wave measuring platform we examine the measured statistics to enquire whether the same behaviour of extremes is observed.

***Comparison with SBWR measurements***

The average ratio of the theoretically estimated $H^*_{\max}$ from Eq. (1) to the observed $H_{max}$ from the 30-minute records is 1.09, indicating that in SBWR measurements the Rayleigh distribution overestimates the maximum wave height by 9%. This confirms the overestimation of $H_{max}$ using the Rayleigh distribution in other platforms (*Forristall*, 1978; *Tayfun*, 1981; *Krogstad*, 1985; *Massel*, 1996; *Nerzic and Prevosto*, 1997; *Mori et al*., 2002; *Casas-Prat and Holthuijsen*, 2010). In Figure 3 the ratio of $H^*_{\max}/H_{max}$ is plotted against *N*, the number of waves in the 30-minute measurement periods. The mean ratio (the black line) increases with increasing *N,* but individual values over 30-minute periods show significant variation, as indicated by the large error bars.

The ratio suggests that for $H_s$>10 m the Rayleigh distribution overestimates $H_{max}$ by 4% on average and for the annual highest sea states, as listed in Table 1, $H_{max}$ is overestimated by 5%. The discrepancy between $H^*_{\max}$ and $H_{max}$ is mainly due to the overestimation of $H_{max}/H_s$ (that will be discussed later) and may also be due to the effect of spectral bandwidth on the estimate of $H_s$.

*Forristall* (1978) suggests an empirical correction coefficient of between 0.90 and 0.96 (depending on *N)* to bring the Rayleigh distribution estimates of $H^*_{\max}$ into better agreement with those from a Weibull distribution. The average ratio of corrected $H^*_{\max}$ to observed $H_{max}$ is 0.99. The ratio against *N* is shown in Figure 3 by the grey line. The trend with *N* and the noise in the individual ratios (see error bars represented by grey squares) remain unaffected by the correction. The discrepancy between the corrected $H^*_{\max}$ and observed $H_{max}$ is significantly reduced, except at the extreme $N$ values where the observed $H_{max}$ are underestimated by the corrected $H^{*}_{\max}$ by about 8% for $N$≈120, and overestimated by a similar amount for $N$≈440 (however this is associated with very low $H_s$ values). Table 1 lists the ratio of $H^{*}_{\max}$ corrected by *Forristall* to that of the observed $H_{max}$ for the largest wave events in each of the 10 years. The mean ratio is 0.97, consistent with the ratio for low $N$ in Figure 3, indicating that under extremely high sea states the measured $H_{max}$ would be underestimated slightly by the use of $H^{*}_{\max}$. However, for the majority of the data the correction brings the observed and theoretical values of the maximum wave height into very close agreement, thus validating the measurements of $H_{max}$ from the SBWR. However it should be noted that the validation concerns the distribution of the values of $H_{max}$ and not their absolute values.

The observed ratios of $H_{max}/H_s$ for the in-situ data are listed in Table 2 and shown in Figure 4. For all the individual 30-minute observations the average (mean) ratio of $H_{max}/H_s$ is 1.53, whilst the median is 1.51. The upper and lower 95% confidence limits are also shown in Figure 4 and have slopes of 1.27 and 1.89 respectively. Table 2 also lists the ratios and confidence limits for various subsets of the in-situ data and demonstrates that the empirical ratio of 1.53 is valid within the confidence limits, even for very large sea states where $H_s$ >10 m. Although the ratio could be expected to vary with $N$ (Eq. (1)), *Feng et al*. (2013) demonstrate that the ratio of $H_{max}/H_s$ has a mean value of 1.53 regardless of $N$, and that this is due to the heterogeneity of sea states encountered. The value of 1.53 is well within the 1.4-1.75 range of values predicted by the Rayleigh and corrected *Forristall* methods. Thus, the relationship between $H_{max}$ and $H_s$ derived from

SBWR wave records is consistent (within the limits of the statistical methods), and the mean does not vary with sea state.

*Myrhaug* and *Kjeldsen* (1986) found a mean ratio of 1.5 when $H_{max}$>5 m for data obtained from 20-minute observational periods on the Norwegian shelf. Their value is ~5% lower than our estimate, but well within our confidence limits.

## 2.3. The NAO index

The North Atlantic Oscillation (NAO) index used here is defined as the normalized sea level pressure difference between the Icelandic Low and the Azores High. This station-based time series of the observed NAO index over 1900-2009 was obtained from the Climate Analysis Section, NCAR, Boulder, USA (http://climatedataguide.ucar.edu). The average value of the NAO index in the boreal winter (December to March) is termed as the winter NAO index here.

The reconstructed winter NAO index for the years 1500 to 2010 from *Luterbacher et al.* (2002) is also used in Section 4. The values of the winter NAO index from the 500-year reconstruction were rescaled to correspond to the range of NAO values from NCAR. The rescaling was done on the basis of a regression coefficient obtained between the two series for the period 1900-1999.

We also use a "future" NAO index derived from the average of the NAO indices from 11 CMIP5 models run under RCP85 for the 21$^{st}$ century (*Taylor et al*., 2012).

## 3. Results

Having established the validity of the measurements from OWS Mike in terms of the $H_{max}$, $H_s$ and their relationships, we now look at the temporal variability of the wave parameters. The mean and maximum values of $H_s$ and $H_{max}$ for each month are shown in Figure 5, with Figure 6 emphasising the interannual variability.

### 3.1. Trends and interannual variability in the wave fields

Over the period 2000-2009 the wave fields exhibit strong seasonal variability (Figure 5), with the monthly mean $H_s$ varying from 1.07 m in the summer to 4.86 m in the winter, and the monthly mean $H_{max}$ varying from 1.68 m in the summer to 7.43 m in the winter. As expected, the largest individual wave heights in each month show more variation than the mean wave heights, with the largest individual $H_{max}$ for each month ranging from 4.10 m to more than 25 m. Note that the highest wave fields in each of the 10 years (see Table 1) happened between November-April. The largest wave height was 25.57 m and occurred on November 11st 2001 when $H_s$ was 15.18 m. There is no statistically significant trend in any of the above seasonal or monthly time series over 2000-2009.

The trends in annual mean and winter mean $H_s$ are 2.03±4.78 and 0.97±7.25 cm/year respectively (Figure 6). Similarly, the trends in annual mean and winter mean $H_{max}$ are 2.61±7.28 and -0.84±13.11 cm/year respectively. None of these trends are statistically significant at the 95% level. This result contrasts with the results for the period 1980-1999 during which a significant increase in annual and winter mean $H_s$ of 3.86±1.67 and 8.48±3.03 cm/year has been observed by *Yelland et al.* (2009) who also used SBWR data from the *Polarfront* (note that $H_{max}$ values were not available prior to 2000).

The combined *Polarfront* time series and the trends are shown in Figure 6. The overall trend in annual mean $H_s$ over 1980-2009 when both observational periods are combined is 2.72±0.88 cm/year. The winter mean trend is 4.63±1.75 cm/year.

For June-August the mean $H_s$ does not show any significant trend.

### 3.2. Relationship of wave field to the NAO

Here we consider the winter averages (December-March) of observed $H_s$ and $H_{max}$ and how these correlate with the large-scale climatic conditions characterized by the winter NAO index. This averaging leaves 10 independent wave field records, hence the correlation coefficient, $r$, must exceed 0.63 to be significant at the 95% level.

The inter-annual variations of winter mean $H_s$ and $H_{max}$ have a clear correspondence with the NAO index, with correlation coefficients of 0.69 and 0.70 respectively. Figure 7 shows the 10-year time series of winter mean $H_s$ and the NAO index. $H_{max}$ is not shown here as it is very similar to $H_s$. For some years (e.g. 2004 and 2007) the correspondence between winter mean $H_s$ and the NAO index appears poor. Figure 7 also shows the time series of wave heights with a 75% level of the exceedance probability: these values are in much better agreement with the NAO index than the average values. To further explain this the correlation coefficients between the NAO index and the wave heights at specific exceedance probabilities are shown in Figure 8. There is no significant correlation for the largest 20% of wave heights. The best correlation is for wave heights that are exceeded 75% of the time ($r$=0.92 for $H_s$ and $r$=0.91 for $H_{max}$).

Figure 9 shows the winter NAO index against the 75$^{th}$ percentile of $H_s$. The plot for $H_{max}$ is very similar and is not shown. A unit change in the NAO index causes a change in the 75$^{th}$ percentile of 0.15±0.05 m for $H_s$ and of 0.21±0.08 m for $H_{max}$. The corresponding value for the mean $H_s$ is 0.15±0.11 m and 0.22±0.17 m for $H_{max}$.

The unit changes are very similar for the mean and 75$^{th}$ percentile values, but the mean values have larger uncertainties due to their poorer correlation with the NAO index.

The similarity between $H_s$ and $H_{max}$ and their correlation with the NAO index arises from their linear relationship (see section 2). Furthermore, the ratios of sensitivities of the two parameters with the change in the NAO ((0.21±0.08)/(0.15±0.05) for the winter average values and (0.22±0.17)/(0.15±0.11) for the winter 75$^{th}$ percentile) confirm that the empirically established relationship $H_{max}$=1.53*$H_s$ with the limits of uncertainty (Section 2.2) can be used to relate $H_{max}$ to the NAO index.

In summary, we confirm that the winter NAO index is correlated with the winter average $H_s$ and $H_{max}$, but is best correlated with wave height values corresponding to the 75% exceedance probability. In contrast, no statistically significant relationship with the NAO index is found for the largest waves (e.g. $r$=0.1 for the largest 1% of $H_s$ in winter).

The lack of correlation between the NAO and the largest waves contrasts with the results of *Wang and Swail* (2001, 2002) who used a wave hindcast and found a correlation value of $r$=0.83 between the NAO index and the largest 1% of $H_s$ in winter during the period 1958-1997 for the North Atlantic. To investigate the discrepancy, we calculate the correlation between $H_s$ derived from the ERA-Interim wave model by ECMWF (*Dee et al.*, 2011) and the winter NAO index for the period 2000-2009. The ERA-Interim model uses data assimilation; however the observations at OWS Mike are not included in the assimilation, thus the two data sources are independent of each other.

We extracted wave height data from the ERA-Interim dataset for the Northeast Atlantic, and found that for the period 2000-2009 the correlation coefficients of the top 1% of winter $H_s$ with the winter NAO values exhibit strong spatial variation (Figure 10). In the Norwegian Sea where OWS Mike operated the top 1% of $H_s$ from the model are not statistically correlated with the NAO index. In contrast, in the region between Iceland and the British Isles the correlation is significant, with the maximum correlation ($r$=0.89) occurring at 63°N, 10.5°W to the Southeast of Iceland. Similarly as results from our observations, at the closest grid point to OWS Mike (66°N, 2°E), the correlation coefficient of the top 15% of winter $H_s$ from ERA-Interim are not significantly correlated to the winter NAO index (grey line in Figure 8), while at 63°N, 10.5°W the winter waves at high probabilities all have a significant (or just below the 95% confidence level) correlation, again indicating that the region between Iceland and the British Isles is the area where the wave fields are fundamentally dominated by the NAO. In Figure 8, the values of correlations from the observed and modeled wave heights agree less well for waves with moderate exceedance probabilities (20-60 %): this is probably due to the different spatial and temporal resolutions of the observations and the model, as well as potential differences in the modeled and observed wind fields. In summary, in the Norwegian Sea the correlation of the NAO with the ERA model wave heights at the higher exceedance probabilities behaves in a similar fashion to those derived from our observations. We therefore consider that the SBWR measurements are consistent with the ERA-Interim model data.

Thus, we can conclude that the apparent discrepancy between our results and those of *Wang and Swail* (2001, 2002) is due to geographical differences and possibly also due to the different period considered. For the area where OWS Mike operated the largest waves are probably associated with the strength of individual storms, a factor which is not reflected by the NAO index in northern middle and high latitudes (*Rogers*, 1997; *Gulev et al.*, 2000; *Walter and Graf*, 2005).

## 4. Discussion

Figure 11 shows time series of the winter mean $H_s$, combined from *Yelland et al* (2009) and the present data, and the winter NAO index. It can be seen that the inter-annual variability of mean $H_s$ in winter is closely related to the variability of the NAO index over the last 2 decades. The correlation coefficient for the whole period 1980-2009 is $r$=0.48, significant at the 95% level. However, during the period 1980 to 1984 the two time series diverge significantly. It is the early part of the time series that dominates the 30-year trend in $H_s$, whereas a 30-year trend over the same period is not found in the NAO index. A number of aspects of the relationship between the NAO index and the wave field in Figure 11 need to be discussed.

The first is the evident discrepancy between the time series for the period 1980 to 1984, which is probably due to other climate aspects rather than the NAO affecting the wind field at OWS Mike. *Gulev et al*. (2000) state that in the Norwegian Sea the inter-annual variability of sea level pressure and other synoptic patterns may not necessarily be correlated with the NAO changes from the early 1970s to the late 1980s. We cannot determine, based on the present data, whether the relationship between the winter NAO index and the mean wave field at OWS Mike is stationary or not, since it might be masked by other large-scale climate phenomena or by synoptic weather systems at smaller scales.

The second issue is the extent to which the NAO changes affected the wave field over the period 1980-2009. To resolve this a linear regression model with mean winter $H_s$ as the dependent variable and the winter NAO index and time as the independent variables is used to separate the changes in $H_s$ caused by the NAO index from those caused by an underlying linear trend for the period 1980-2009. The model accounts for 74% of the observed variance. The NAO index accounts for 23% of the variability in the mean wave fields, with the sensitivity being 0.28±0.12 m per unit NAO index, whereas a trend of 4.63±1.75 cm/year accounts for 51% of the variability. This indicates that in the Norwegian Sea there is a pronounced trend in winter wave height measurements over those 30 years that is not explained (linearly) by the NAO index changes. This is in agreement with the results of *Woolf et al.* (2002) who also suggest a partial contribution of the NAO index to the variability in $H_s$ but note that other large-scale atmospheric patterns (e.g. the East Atlantic Pattern) may also be contributing to mean wave field changes in the Northeastern Atlantic. The Arctic Oscillation may also be relevant in explaining the changes in the wave field since this has been found to be associated with storms occurring in northern middle and high latitudes and accounts for their occurrence better than the NAO (*Walter and Graf,* 2005).

The third point is the variation of $H_{max}$ for the period 1980-2009. Although we have $H_{max}$ data for the period 2000-2009, no $H_{max}$ data were recorded prior to 2000. If we assume that the established empirical relationship between $H_{max}$ and $H_s$ is stationary, the inter-annual variability of $H_{max}$ at OWS Mike can be extended backwards for the period 1980-1999 based on the $H_s$ observations. Changes in annual mean and winter mean $H_{max}$ for 1980-2009 are thus estimated to be 4.13±1.35 cm/year and 7.09±2.68 cm/year respectively. Thus we estimate a total change in annual mean $H_{max}$ of about 1.24 m over the last 30 years, and a total change in winter mean $H_{max}$ of about 2.13 m during the same period.

The fourth point is the expected natural variability of the wave field. We have shown from observations at OWS Mike that the NAO index could explain part of the interannual variability of the mean wave field at this location. Thus this permits the possibility of assessing longer-term interannual variability of this part of the wave field based on historic or predicted values of the NAO index on the assumption that the relationship remains stationary in time. When assessing historic and future wave fields using the NAO index it should be kept in mind that other factors, e.g. global climate or the East Atlantic Pattern, may also be involved, as discussed above. The reconstructed winter NAO index for the period 1500-2010 (*Luterbacher et al.,* 2002) has been used to estimate changes in winter mean $H_s$ and $H_{max}$. The historic winter NAO index (after being re-scaled to correspond to the NAO index used over the later observational period) varies between -5.00 and 4.48. This corresponds to a total range of 1.42 m in the winter mean $H_s$ (Figure 12a) based on the results in Section 3.2. A variability of 1.42 m in $H_s$ translates to a mean value or an upper confidence limit for the variability in $H_{max}$ of 2.17 m or 3.10 m using the relationships established between $H_s$ and $H_{max}$ in Section 2.2.

The 500-year reconstruction of the NAO index includes long periods of several decades of persistent change during which the index tends to increase/decrease steadily. Since we have a 30-year in-situ record with a strong trend we calculated trends in the interannual variations of the wave field (reconstructed from the

500-year NAO index) using centered and overlapping 30-year segments (Figure 12b). A large increase in the reconstructed $H_s$ is found for the period 1954-1995, which includes the periods of increasing mean wave height during 1962-1986 to the west of the British Isles and also during 1965-1993 in the Norwegian Sea, as previously identified from in-situ and visual wave observations respectively (*Bacon and Carter,* 1993; *Gulev and Hasse*, 1999). This increase in the reconstructed $H_s$ for 1954-1995 is consistent with the tendency in the Norwegian Sea during 1957-2002 derived from ERA-40 (*Semedo et al*., 2011). A large decreasing trend is found during the period 1903-1949. However, it is notable that none of the 30-year segments from the 500-year period show trends greater than those found from the SBWR data for the last 3 decades, that is, 4.63 cm/year for $H_s$. Therefore we conclude that the recently observed changes in the wave climate are not within the natural variability of decadal trends caused by NAO index variations alone.

Finally we discuss the possibility of using the results of this study for estimating future changes in the wave parameters in the region. Again the underlying assumption is that the linear relationships identified will remain unaltered in the future. *Wang and Swail* (2006) assessed projections from different climate models and conclude that the uncertainty of future wave fields due to the different scenarios is much less than that due to differences among climate models. In the present study the future winter NAO index was obtained by evaluating the difference between the normalized sea level pressure anomalies at Gibraltar and Iceland from different climate models forced by increasing greenhouse gas concentrations.

We examined the sea level pressure fields in 11 different models that have been made available as part of the 5$^{th}$ Coupled Model Intercomparison Project (CMIP5) (*Taylor et al*., 2012). The selected models (see Table 3) were those that were the first to make many fields easily available for both historic and future scenarios. We analysed the output for the 21$^{st}$ century under scenario RCP85, which corresponds to the most extreme greenhouse warming conditions. For each model, sea level pressure (SLP) was extracted for the atmospheric grid cells corresponding to Gibraltar and Reykjavik, and a winter NAO index was calculated that was consistent with the definitions used for the station-based historical records obtained from NCAR. The derived NAO time series for each model had a variability (standard deviation) of about one for both the historical period (1850-2005) and for that after 2050. This shows that the models exhibit future interannual variations of SLP that have a similar magnitude to historic variations, i.e. they show no pronounced change in intensity. Although some models do show a difference between the mean NAO values for the historic and future periods, there is no consistent picture. This indicates that only small changes in the atmospheric pressure are projected by the models. Consequently, the majority of the models (10 out of 11) suggest that the mean NAO index for the end of the 21$^{st}$ century will be within 0.3 units of that for the end of the 20$^{th}$ century, with the average change for the ensemble being zero. Our assessment of the future NAO index is consistent with those from CMIP2 models in that the response of the NAO to greenhouse warming is model-dependent but generally very limited (*Stephenson et al.,* 2006). In contrast, *Gillett and Fyfe* (2013) examined SLP averaged over large regions and found a positive trend in the NAO index for RCP45 CMIP5 models. However, using a different definition of NAO index based on the height of the 500 mb surface in CMIP5 models, *Cattiaux et al*. (2013) found that the changes in the NAO are model-dependent and that most of the CMIP5 models suggest an increase in the frequency of the negative NAO state. Whether this difference between CMIP2 and CMIP5 models is due to the variable or climate scenarios selected for the NAO analysis, or due to changes in the modeling of specific processes (in particular the addition of sea ice) is something that remains to be resolved (*Cattiaux et al*., 2013).

The stability of the winter NAO index in the future leads to the conclusion that the wave field is not expected to change as a result of the NAO index changes. However, as noted above, other processes in the Norwegian Sea that cannot be fully captured by the NAO index are also relevant in determining the future mean wave field, most notable of which is the possibility of stronger storms as a result of greenhouse warming (*Emanuel*, 1987).

*Hemer et al.* (2013) have found from a multi-model ensemble of wave-climate projections that the winter mean $H_s$ will decrease overall by ~5% in the North Atlantic but increase by 1-2% in the Norwegian Sea in the future (2070-2100) compared to the present mean wave field (1979-2009). The wave height trends seen in their model agree within 95% confidence limits with those from altimetry observations for the vast majority of the global ocean for the period 1992-2003. However, the model trends disagree with the altimeter observations for some areas of the North Atlantic and the Norwegian Sea (Figure SM5d in *Hemer et al.* (2013)). In addition, *Hemer et al*. (2013) find that more than half of CMIP3 models project a positive trend in the NAO index, but they do not observe a projected increase in the ensemble mean wave heights in the northern North Atlantic, contrary to what might be expected with a projected strengthening of NAO.

Our results show that the effect of the NAO on the wave field explains little of the observed mean trend, and the CMIP5 analysis indicates no significant change in the future NAO index. Therefore, in our view, the contradiction identified by *Hemer et al.* (2013) between a future NAO increase in CMIP3 and the reduction in mean wave heights they predict in most areas of the North Atlantic indicates that the projected changes are not related to the NAO variability but to other aspects of the wind field, and possibly to changes in other atmospheric modes.

## 5. Conclusions

Our analysis of 10 years of 30-minute measurements from a SBWR at Ocean Weather Station Mike was used to establish the statistical characteristics of $H_s$ and $H_{max}$. These were consistent with theoretical distributions of ocean waves that have been confirmed on the basis of observations derived from other wave platforms, but not previously for the SBWR. The close similarity between the observations from the SBWR and the theoretical estimations, including the empirical corrections normally used for wave measurements, confirms the reliability of the measurements at OWS Mike and permits the use of the observations in the analysis of the mean and extreme waves.

For the 30-minute measurement periods, $H_{max}$=1.53*$H_s$ with the 95% confidence limits given by 1.27*$H_s$ and 1.89*$H_s$. These empirical relationships allow $H_{max}$ to be estimated from observed or predicted $H_s$.

The observations showed no statistically significant trend in $H_s$ or $H_{max}$ over the period 2000-2009. By combining our data with earlier measurements we updated the long-term trends of annual mean and winter (December-March) mean $H_s$ in the region for the period 1980-2009 to 2.72±0.88 and 4.63±1.75 cm/year. Thus, a significant change of 0.82 m in annual $H_s$ and 1.39 m in winter $H_s$ over the 30 years of observations was confirmed. The trends in annual mean and winter mean $H_{max}$ over those 30 years were estimated to be 4.13 cm/year and 7.09 cm/year respectively. The largest $H_{max}$ observed in the period 2000-2009 was 25.57 m and occurred in a wave field with an $H_s$ of 15.18 m.

The winter mean wave fields are significantly correlated with the winter NAO index over 2000-2009, with sensitivities of 0.15 and 0.22 m per unit NAO index for $H_s$ and $H_{max}$ respectively. For the extended time series (1980-2009) the sensitivity of $H_s$ is 0.28 m per unit NAO index. However over the three decades the NAO index explains only 23% of the variability in $H_s$ while a linear trend explains 51% of the variability. The NAO index accounts for 55% of the variability for the period 2000-2009 when there is no overall trend present.

The relationship of the wave field at OWS Mike with the NAO index over 2000-2009 is dominated by the association of the NAO index with the wave heights corresponding to the middle-to-high exceedance probabilities. The correlation with the NAO for the largest 20% of the waves is not statistically significant. The lack of correlation at OWS Mike is consistent with ERA-Interim results for the largest wave fields in the same region. We also confirmed that the area between Iceland and the British Isles is the area where the largest waves are dominated by the NAO. A companion paper (*Feng et al.*, 2013) examines the persistence of the wave field and found that it is the duration of the moderate wave conditions that is most closely connected to the state of the NAO, rather than the duration of extreme conditions.

The natural variability in winter wave fields for the past 5 centuries in the region was found to be 1.42 m for $H_s$ and up to 3.10 m for $H_{max}$. Here $H_{max}$ was estimated using its empirical relationship with $H_s$ that was confirmed by the correlations of the two wave parameters with the NAO index over 2000-2009. The reconstructed wave fields for the past 500 years do not include any 30-year period where the changes in the winter wave fields exceed the increase observed during the last 3 decades.

CMIP5 climate model projections showed no changes in the winter NAO index over the 21st century, thus no appreciable changes in the winter wave fields associated with the winter NAO index are to be expected. However as the largest waves are not correlated with the NAO index and the changes in the mean wave field over the last 3 decades are only partly associated with the NAO index, future changes in the largest waves and also in the mean wave field in this region cannot be ruled out.

## Acknowledgements

This research is funded by Lloyd's Register Foundation, which supports the advancement of engineering-related education, and funds research and development that enhances safety of life at sea, on land and in the air. This research is also supported by National Natural Science Foundation of China (Grant No. 51109075). Thanks to Knut Iden of the Norwegian Meteorological Institute, DNMI, for supplying the wave measurements, and to the WCRP Working Group on Coupled Modelling, organisers of the 5th Coupled Model Intercomparison Project and to ERA-Interim project of ECMWF, for making so much model output widely available.

## References

Bacon, S., Carter, D.J.T., 1993. A connection between mean wave height and atmospheric pressure gradient in the North Atlantic. Int. J. Climatol. 13, 423–436. http://dx.doi.org/10.1002/joc.3370130406.

Bretschneider, C. L., 1959. Wave variability and wave spectra for wind-generated gravity waves. Tech. Memo. 118U.S. Beach Erosion Board, Washington, D.C..

Casas-Prat, M., Holthuijsen, L.H., 2010. Short-term statistics of waves observed in deep water. J. Geophys. Res. 115, C09024. http://dx.doi.org/10.1029/2009JC005742.

Cattiaux, J., Douville, H., Peings, Y., 2013. European temperatures in CMIP5: origins of present-day biases and future uncertainties. Climate Dynamics, 1-19. http://dx.doi.org/ 10.1007/s00382-013-1731-y.

Clayson, C.A., 1997. Intercomparison between a WS Ocean Systems Ltd. Mk IV shipborne wave recorder (SWR) and a Datawell Waverider (WR) deployed from DNMI ship Polarfront during March-April 1997. Southampton Oceanography Centre, Southampton, UK, 26pp. (Unpublished report).

Crisp, G.N., 1987. An experimental comparison of a shipborne wave recorder and a waverider buoy conducted at the Channel Lightvessel. Wormley, UK, Institute of Oceanographic Sciences, 181pp. (Institute of Oceanographic Sciences Report, (235) ).

Dee, D.P., Uppala, S.M., Simmons, A.J., Berrisford, P., Poli, P., Kobayashi, S., Andrae, U., et al., 2011. The ERA-Interim reanalysis: configuration and performance of the data assimilation system. Q. J. R. Meteorol. Soc. 137(656), 553–597. http://dx.doi.org/10.1002/qj.828.

Dobson, E., Monaldo, F., Goldhirsh, J., Wilkerson, J., 1987. Validation of Geosat altimeter-derived wind speeds and significant wave heights using buoy data. J. Geophys. Res. 92(C10), 10719–10731. http://dx.doi.org/10.1029/JC092iC10p10719.

Emanuel, K.A., 1987. The dependence of hurricane intensity on climate. Nature. 326, 483-485. http://dx.doi.org/10.1038/326483a0.

Feng X., Tsimplis ,M.N., Quartly, G.D., Yelland, M.J., 2013. Wave height analysis from 10 years of observations in the Norwegian Sea, Continental Shelf Research. http://dx.doi.org/10.1016/j.csr.2013.10.013.

Forristall, G.Z., 1978. On the statistical distribution of wave heights in a storm. J. Geophys. Res. 80, 2353–2358. http://dx.doi.org/10.1029/JC083iC05p02353.

Gemmrich, J., Garrett, C., 2011. Dynamical and statistical explanations of observed occurrence rates of rogue waves. Nat. Hazards Earth Syst. Sci. 11, 1437–1446. http://dx.doi.org/ 10.5194/nhess-11-1437-2011.

Gillett, N.P., Fyfe, J.C., 2013. Annular mode changes in the CMIP5 simulations. Geophysical Research Letters, 40, 1189-1193. http://dx.doi.org/10.1002/grl.50249

Graham, C., Verboom, G., Shaw, C.J., 1978. Comparison of shipborne wave recorder and waverider buoy data used to generate design and operational planning criteria. Proceedings 16th International coastal Engineering Conference, Hamburg, Am. Soc. Cir. Eng., New York, N.Y., p97-113.

Gulev, S.K., Hasse, L., 1999. Changes of wind waves in the North Atlantic over the last 30 years. Int. J. Climatol. 19, 720–744. http://dx.doi.org/10.1002/(SICI)1097-088(199908)19:10<1091::AID-JOC403>3.0.CO;2-U.

Gulev, S.K., Zolina, O., Reva, Y., 2000. Synoptic and subsynoptic variability in the North Atlantic as revealed by the Ocean Weather Station data. Tellus A. 52: 323–329. http://dx.doi.org/ 10.1034/j.1600-0870.2000.d01-6.x.

Hemer, M.A., Fan, Y., Mori, N., Semedo, A., Wang, X.L., 2013. Projected changes in wave climate from a multi-model ensemble. Nature Clim. Change. http://dx.doi.org/10.1038/nclimate1791.

Holliday, N.P., Yelland, M.J., Pascal, R., Swail, V.R., Taylor, P.K., Griffiths, C.R., Kent, E., 2006. Were extreme waves in the Rockall Trough the largest ever recorded? Geophys. Res. Lett. 33, L05613. http://dx.doi.org/10.1029/2005GL025238.

Hurrell J.W., Van Loon, H., 1997. Decadal variations in climate associated with the north Atlantic Oscillation. Clim. Change. 36, 301 – 326. http://dx.doi.org/ 10.1023/A:1005314315270.

Hurrell, J.W., 1995. Decadal trends in the North Atlantic Oscillation: Regional temperatures and precipitation. Science. 269, 676–679. http://dx.doi.org/ 10.1126/science.269.5224.676.

Izaguirre, C., Mendez, F.J., Menendez, M., Luceño, A., Losada, I.J., 2010. Extreme wave climate variability in southern Europe using satellite data. J. Geophys. Res. 115(C4), C04009. doi:10.1029/2009JC005802.

Krogstad, H.E., 1985. Height and period distributions of extreme waves, Appl. Ocean Res. 7 (3), 158–165. http://dx.doi.org/ 10.1016/0141-1187(85)90008-2.

Kushnir, Y., Cardone, V.J., Greenwood, J.G., Cane, M.A., 1997. The recent increase in North Atlantic wave heights. J. Clim. 10, 2107–2113. http://dx.doi.org/ http://dx.doi.org/10.1175/1520-0442(1997)010<2107:TRIINA>2.0.CO;2.

Longuet-Higgins M.S., 1952. On the statistical distribution of the heights of sea waves. J. Mar. Res. 11(3), 1245-1266.

Luterbacher, J., Xoplaki, E., Dietrich, D., Jones, P.D., Davies, T.D., Portis, D., Gonzalez-Rouco, J.F., von Storch, H., Gyalistras, D., Casty, C., Wanner, H., (2002), Extending North Atlantic Oscillation reconstructions back to 1500. Atmos. Sci. Lett., 2, 114-124. http://dx.doi.org/10.1006/asle.2001.0044.

Massel, S.R., 1996. Ocean Surface Waves: Their Physics and Prediction, 11, World Scientific, Singapore.

Mori N., Liu, P.C., Yasuda, T., 2002. Analysis of freak wave measurements in the Sea of Japan. Ocean Eng. 29, 1399-1414. http://dx.doi.org/10.1016/S0029-8018(01)00073-7.

Myrhaug, D., Kjeldsen, S.P., 1986). Steepness and asymmetry of extreme waves and the highest waves in deep water. Ocean Eng. 13(6), 549–568. http://dx.doi.org/10.1016/0029-8018(86)90039-9.

Nerzic, R., Prevosto, M., 1997. A Weibull-Stokes model for the distribution of maximum wave and crest heights. Proceedings of the 7th International Offshore and Polar Engineering Conference, Honolulu, Hawaii, 3, 367-377.

Ochi, M.K., 1998. Ocean Waves: The Stochastic Approach, Ocean Technology Series, Vol. 6. Cambridge University Press, p81-83.

Osborn, T.J., Briffa, K.R., Tett, S.F.B., Jones, P.D., Trigo, R.M., 1999. Evaluation of the North Atlantic Oscillation as simulated by a coupled climate model. Clim. Dyn. 15, 685–702. http://dx.doi.org/10.1007/s003820050310.

Phillips, O.M., 1977. The Dynamics of the Upper Ocean. Cambridge University Press, 336pp.

Pitt, E.G., 1991. A new empirically-based correction procedure for ship-borne wave recorder data. Appl. Ocean Res. 13, 162–174.

Rogers, J.C., 1997. North Atlantic storm track variability and its association to the North Atlantic Oscillation and climate variability of northern Europe. J. Clim. 10, 1635–1647. http://dx.doi.org/10.1175/1520-0442(1997)010<1635:NASTVA>2.0.CO;2.

Sarpkaya, T., Isaacson, M., 1981. Mechanics of wave forces on offshore structures. Van Nostrand Reinhold, New York, 651pp.

Semedo, A., Sušelj, K., Rutgersson, A., Sterl, A., 2011. A global view on the wind sea and swell climate and variability from ERA-40. J. Clim. 24, 1461-1479. http://dx.doi.org/10.1175/2010JCLI3718.1.

Slunyaev, A.V., Sergeeva, A.V., 2012. Stochastic simulation of unidirectional intense waves in deep water applied to rogue waves. JETP letters 94(10), 779-786. http://dx.doi.org/10.1134/S0021364011220103.

Stansell, P., 2004. Distributions of freak wave heigths measured in the North Sea. Appl. Ocean Res. 26 (1–2), 35–48. http://dx.doi.org/ 10.1016/j.apor.2004.01.004.

Stephenson, D. B., Pavan, V., Collins, M., Junge, M. M., Quadrelli, R., 2006. North Atlantic Oscillation response to transient greenhouse gas forcing and the impact on European winter climate: a CMIP2 multi-model assessment. Climate Dynamics, 27(4), 401-420. http://dx.doi.org/ 10.1007/s00382-006-0140-x.

Sterl, A., Komen, G.J., Cotton, P.D., 1998. Fifteen years of global wave hindcasts using winds from the European Centre for Medium-Range Weather Forecasts reanalysis: Validating the reanalyzed winds and assessing the wave climate. J. Geophys. Res. 103(C3), 5477–5492. http://dx.doi.org/10.1029/97JC03431.

Sverdrup, H.U., Munk, W.H., 1947. Wind, Sea, and Swell: Theory of Relations for Forecasting. U.S. Navy Dept., Hydrographic Office, H.O. Pub. No. 601, 44pp.

Tayfun, M.A., 1981. Distribution of crest-to-trough wave heights. J. Waterway, Port, Coastal, Ocean Eng. 107(3), 149-158.

Tayfun, M.A., 1983. Nonlinear effects on the distribution of crest-to-trough wave heights. Ocean Eng. 10(2), 97-1.

Taylor, K.E., Stouffer, R.J., Meehl, G.A., 2012. An overview of CMIP5 and the experiment design. Bull. Amer. Meteor. Soc. 93, 485-498. http://dx.doi.org/10.1175/BAMS-D-11-00094.1.

Tsimplis, M.N., Woolf, D.K., Osborn, T.J., Wakelin, S., Wolf, J., Flather, R., Shaw, A.G.P., et al., 2005. Towards a vulnerability assessment of the UK and northern European coasts: the role of regional climate variability. Phil. Trans. Roy. Soc. A. 363, 1329–58. http://dx.doi.org/10.1098/rsta.2005.1571.

Tucker, M.J., Pitt, E.G., 2001. Waves in Ocean Engineering, Ocean Eng. Book Ser., Elsevier, New York, vol. 5, pp81, 521.

Vandever, J., Siegel, E., Brubaker, J., Friedrichs, C., 2008. Influence of spectral width on wave height parameter estimates in coastal environments. J. Waterway, Port, Coastal, Ocean Eng. 134(3), 187–194. http://dx.doi.org/ 10.1061/(ASCE)0733-950X(2008)134:3(187).

Walter, K., Graf, H.F., 2005. The North Atlantic variability structure, storm tracks, and precipitation depending on the polar vortex strength. Atmos. Chem. Phys. 5, 239-248. http://dx.doi.org/10.5194/acp-5-239-2005.

Wang, X.L., Swail, V.R., 2001.Changes of extreme wave heights in Northern Hemisphere oceans and related atmospheric circulation regimes. J. Clim. 14, 2204–2221. http://dx.doi.org/ 10.1175/1520-0442(2001)014<2204:COEWHI>2.0.CO;2.

Wang, X.L., Swail, V.R., 2002. Trends of Atlantic wave extremes as simulated in a 40-year wave hindcast using kinematically reanalyzed wind fields. J. Clim. 15, 1020–1035. http://dx.doi.org/ /10.1175/1520-0442(2002)015<1020:TOAWEA>2.0.CO;2.

Wang, X.L., Swail, V.R., 2006. Climate change signal and uncertainty in projections of ocean wave heights. Clim. Dynam. 26, 109–126. http://dx.doi.org/ 10.1007/s00382-005-0080-x.

Wang, X.L., Zwiers, F.W., Swail, V.R., 2004. North Atlantic Ocean wave climate change scenarios for the twenty-first century. J. Clim. 17, 2368-2383. http://dx.doi.org/10.1175/1520-0442(2004)017<2368:NAOWCC>2.0.CO;2.

Wolf, J., Woolf, D.K., 2006. Waves and climate change in the north-east Atlantic. Geophys. Res. Lett. 33, L06604. http://dx.doi.org/10.1029/2005GL025113.

Woolf, D.K., Challenor, P.G., Cotton, P.D., 2002. Variability and predictability of the North Atlantic wave climate. J. Geophys. Res. 109, 3145-3158. http://dx.doi.org/10.1029/2001JC001124.

Yelland M.J., Holliday, N.P., Skjelvan, I., Osterbus, S., Conway, T.J., 2009. Continuous observations from the weather ship Polarfront at Station M. Proceedings of OceanObs'09: Sustained Ocean Observations and Information for Society (Annex), Venice, Italy, Hall, J., Harrison, D.E. and Stammer, D., Eds., ESA Publication WPP-306.

Ying, L. H., Kaplan, L., 2012. Systematic study of rogue wave probability distributions in a fourth-order nonlinear Schrödinger equation. Journal of Geophysical Research 117, C08016. http://dx.doi.org/10.1029/2012JC008097.

**FIGURES:**

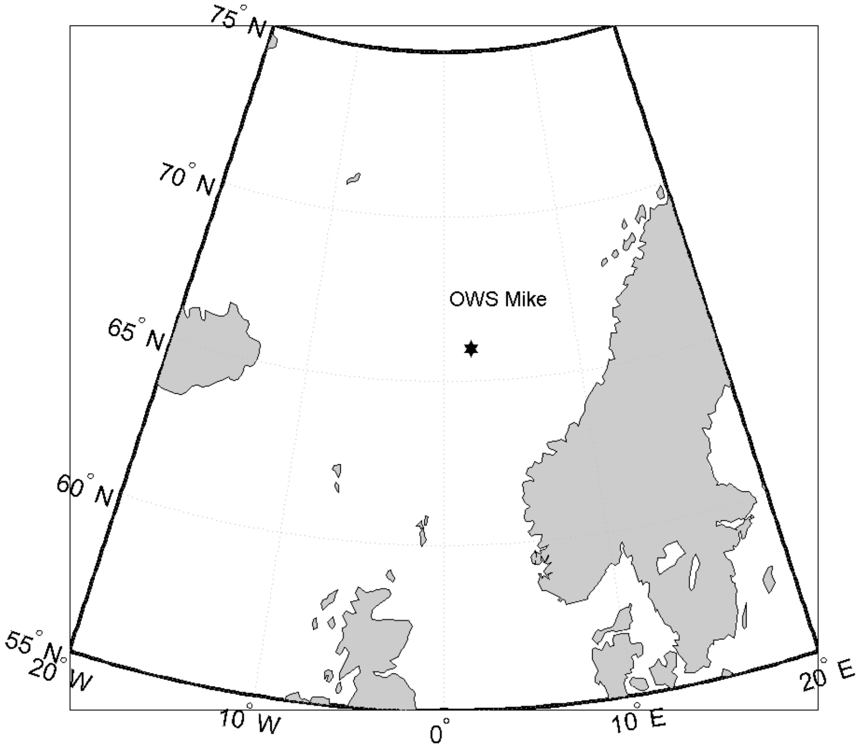


**Figure 1. Location of Ocean Weather Station Mike (66°N, 2°E).**

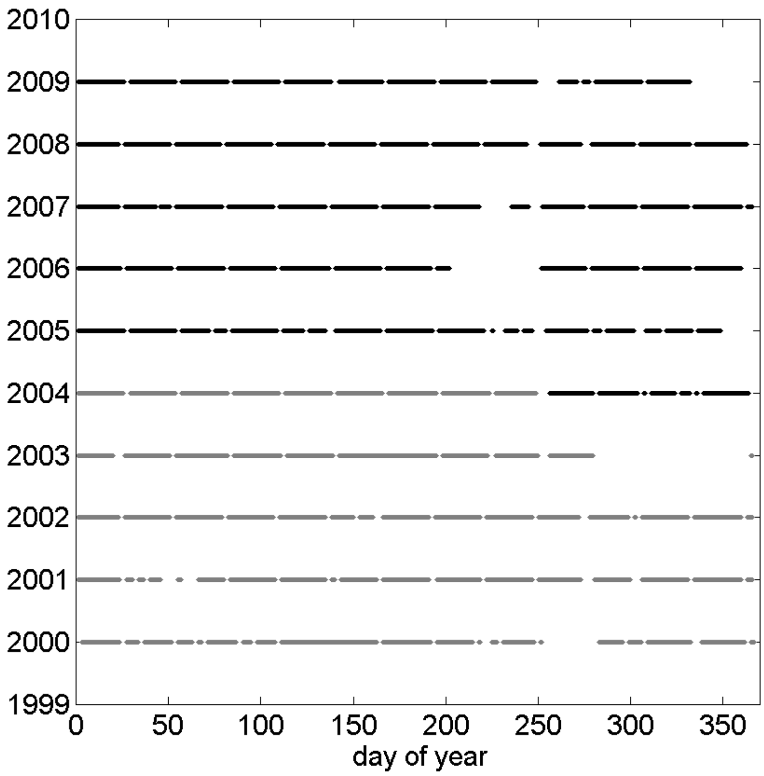


**Figure 2. Quality-controlled SBWR data from OWS Mike during 2000-2009. Grey lines indicate that the observing frequency was every 90 minutes, and black every 45 minutes.**

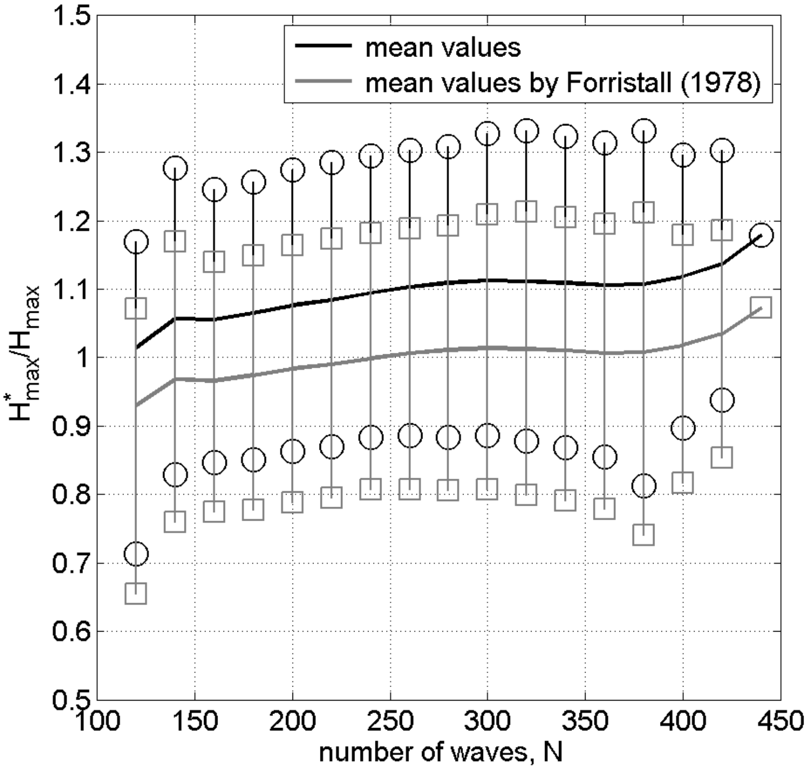


**Figure 3. Ratios of the estimated $H^*_{max}$ to the observed $H_{max}$ against the number of waves, *N*, in the 30-minute records. Ratios for $H^*_{max}$ estimated from both Rayleigh (black line) and corrected Rayleigh (grey line) [*Forristall,* 1978] distributions are shown. Error bars represent the 95% confidence limits for both estimates (black circles and grey squares respectively).**

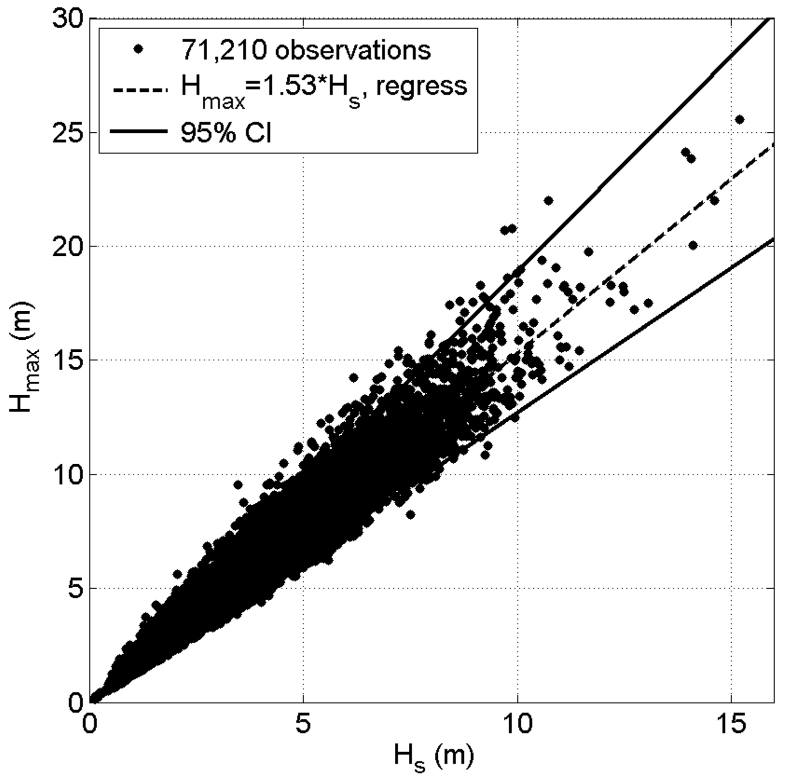


**Figure 4. Scatter plot of $H_{max}$ versus $H_s$ for all the individual 30-minute wave records. The dashed lines show the mean ratio of $H_{max}/H_s$, and the solid lines indicate the upper and lower limits at the 95% confidence level. The ratios are listed in Table 2.**

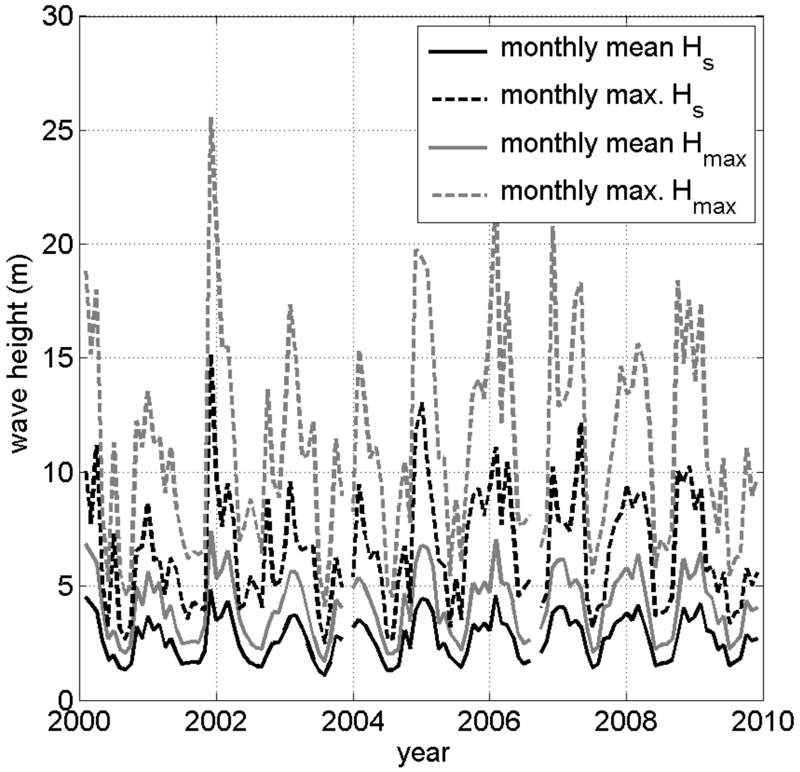


**Figure 5. Monthly values of mean *$H_s$*, largest *$H_s$*, mean *$H_{max}$* and largest *$H_{max}$* during 2000-2009.**

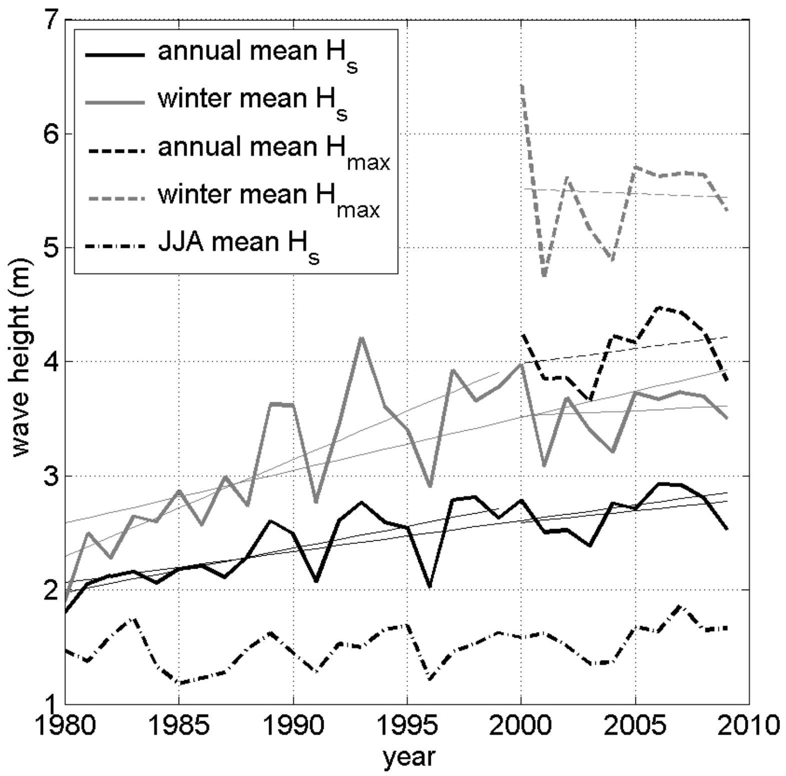


**Figure 6. Annual, winter and summer (JJA) mean *$H_s$* and *$H_{max}$* (when available) during 1980-2009 at OWS Mike, along with linear trends (over periods 1980-1999, 2000-2009 and1980-2009 separately). Winter and JJA represent the time periods December-March and June-August respectively. The *$H_s$* data for 1980-1999 were previously shown in *Yelland et al* [2009].**

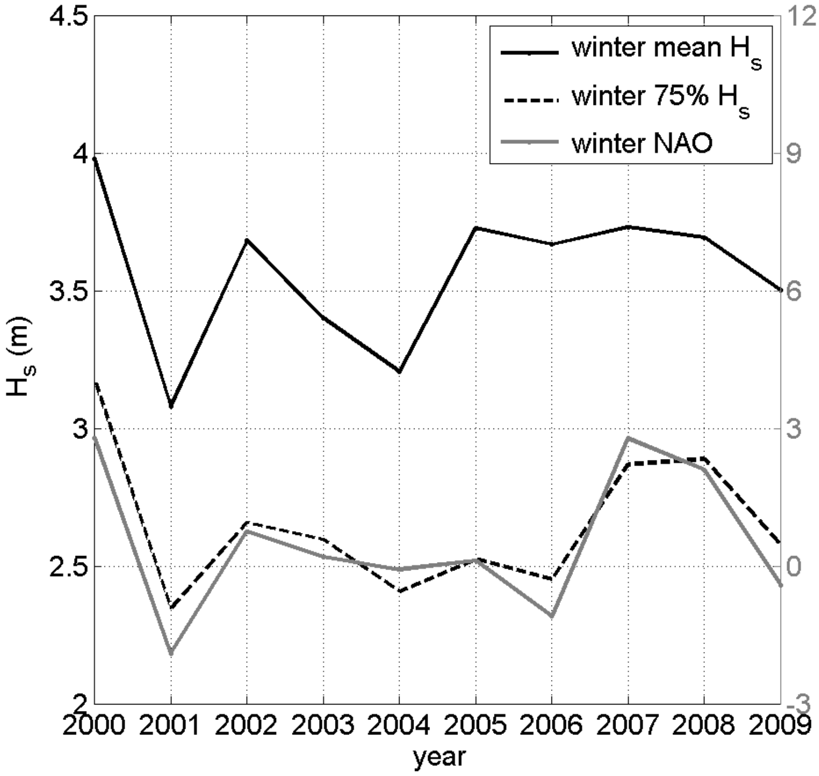


**Figure 7. Time series of winter NAO index (solid grey line) and winter mean $H_s$ (solid black line). The dashed black line indicates the 75th percentile of winter $H_s$.**

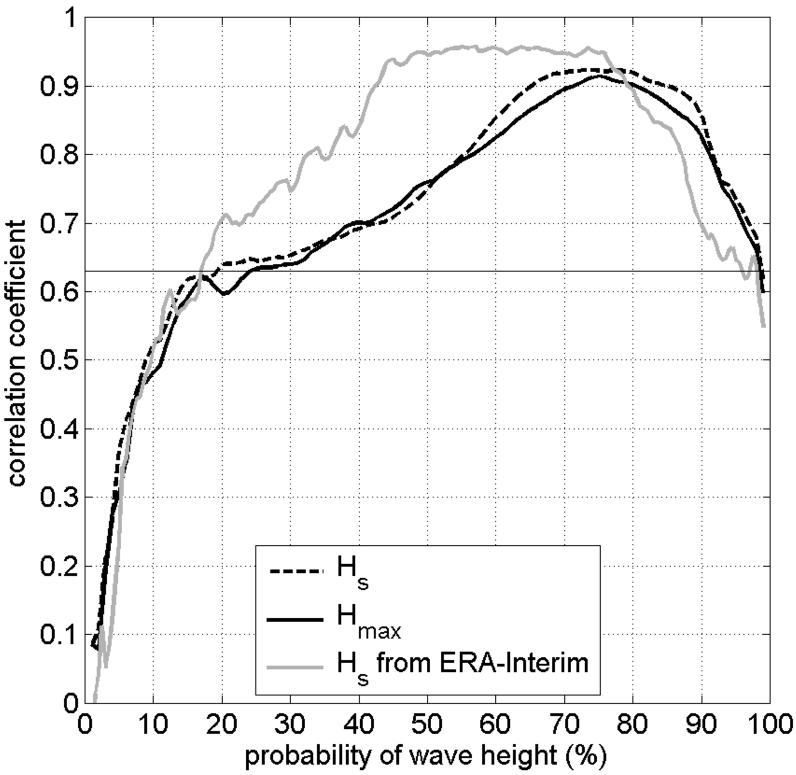


**Figure 8. Correlation coefficients of winter NAO index with winter wave heights at varying exceedance levels for 2000-2009: black dashed and black solid lines for observed $H_s$ and $H_{max}$ respectively; grey solid line for the model $H_s$ at the closest grid point of ERA-Interim dataset. The thin solid line corresponds to correlations with the 95% significance level.**

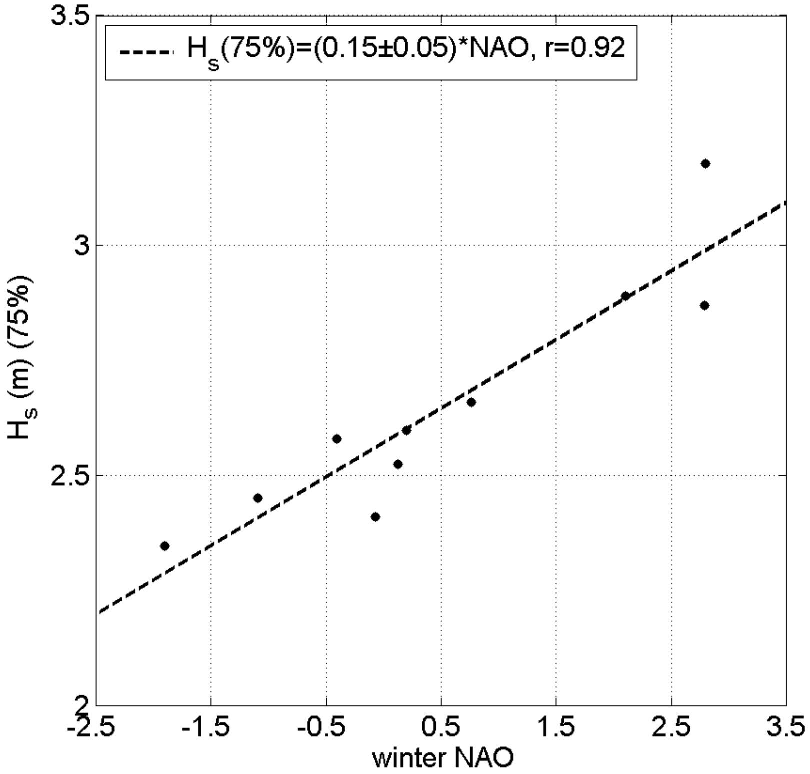


**Figure 9. Scatter plots of winter NAO index versus the 75th percentile of winter $H_s$. The dashed line indicates the linear regression, with coefficients given in the legend.**

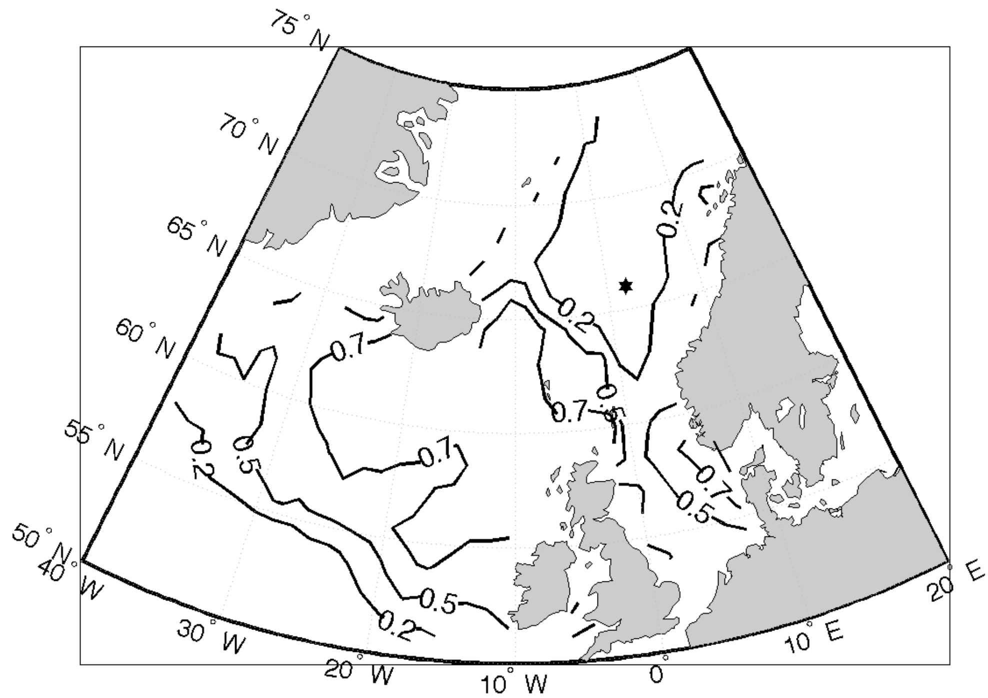


**Figure 10. Contour map of correlation coefficients of winter NAO index with the 1st percentile of winter $H_s$ for 2000-2009. The wave data are derived from ERA-Interim dataset. The star indicates the position of OWS Mike.**

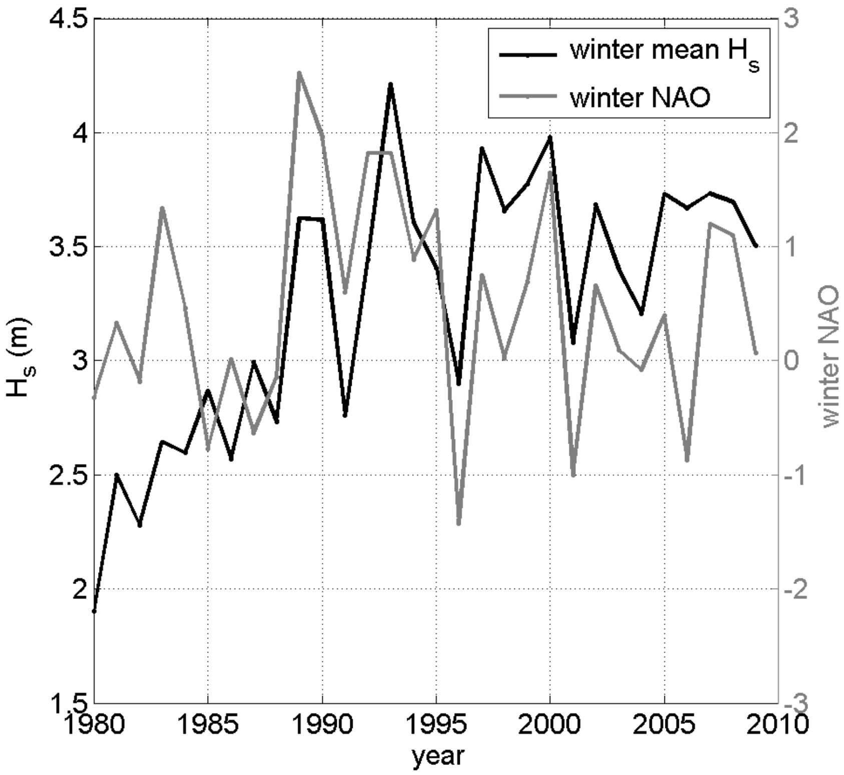


**Figure 11. Time series of winter mean $H_s$ and winter NAO index for 1980-2009.**

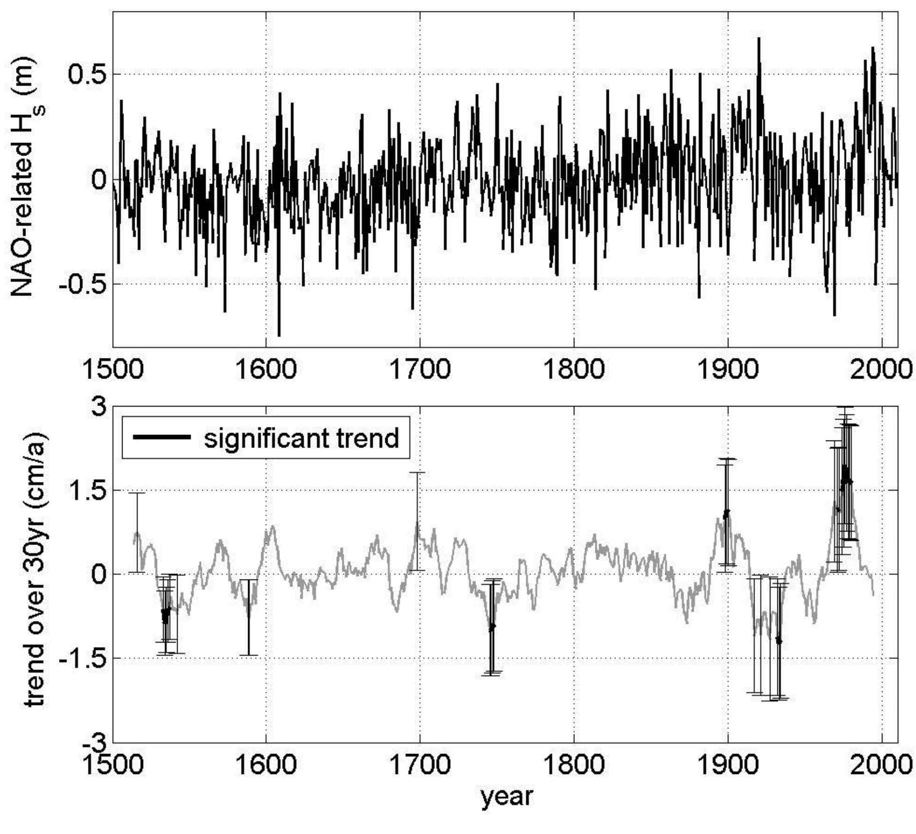


**Figure 12. (a) Annual anomaly of winter mean $H_s$ that is related to the NAO in the past 5 centuries using the reconstructed NAO index (*Luterbacher et al.*, 2002), and (b) its corresponding trends from centered and overlapping 30-year segments (grey line). The trends that are significant at the 95% confidence level are highlighted by bold black line with error bars. Note that this analysis only shows that portion of the mean $H_s$ variability related to the NAO.**

**TABLES:**

**Table 1. The highest individual wave events in each year for the period 2000-2009.**

| *Time* | *$H_s$ (m)* | *$H_{max}$ (m)* | *N* | $H^*_{max}$ *by Rayleigh (m)* | $H^*_{max}$ *by Forristal (m)* | $\frac{H_{max}}{H_s}$ | $\frac{H^*_{max}(Forristal)}{H_{max}}$ |
|---|---|---|---|---|---|---|---|
| ***0/03/07/09:00*** | 11.18 | 18.01 | 122 | 17.25 | 15.82 | 1.61 | 0.88 |
| ***2001/11/11/08:00*** | 15.18 | 25.57 | 142 | 23.80 | 21.81 | 1.68 | 0.85 |
| ***2002/02/24/05:00*** | 9.50 | 12.68 | 160 | 15.07 | 13.80 | 1.33 | 1.09 |
| ***2003/01/30/11:00*** | 9.57 | 13.34 | 163 | 15.21 | 13.92 | 1.39 | 1.04 |
| ***2004/12/16/02:45*** | 13.06 | 17.51 | 146 | 20.54 | 18.81 | 1.34 | 1.07 |
| ***2005/01/31/04:15*** | 10.30 | 15.01 | 161 | 16.36 | 14.97 | 1.46 | 1.00 |
| ***2006/01/11/20:00*** | 11.10 | 18.31 | 160 | 17.61 | 16.12 | 1.65 | 0.88 |
| ***2007/04/10/22:30*** | 12.20 | 18.31 | 160 | 19.35 | 17.71 | 1.50 | 0.97 |
| ***2008/11/21/11:15*** | 10.26 | 15.63 | 162 | 16.30 | 14.92 | 1.52 | 0.95 |
| ***2009/01/16/08:15*** | 9.18 | 13.84 | 162 | 14.57 | 13.34 | 1.51 | 0.96 |
| ***Average*** | 11.15 | 16.82 | 154 | 17.61 | 16.12 | 1.50 | 0.97 |

**Table 2. Observed ratios of $H_{max}$ to corresponding $H_s$ in different states.**

| *Conditions* | *$H_{max}/H_s$* | | |
|---|---|---|---|
| | *Regression* | *Lower limit** | *Upper limit** |
| ***All*** | 1.53 | 1.27 | 1.89 |
| ***Winter*** | 1.52 | 1.28 | 1.88 |
| ***$H_{max}$>5m*** | 1.57 | 1.30 | 1.94 |
| ***$H_s$>10m*** | 1.53 | 1.34 | 1.88 |
| ***Annual largest $H_s$*** | 1.50 | 1.33** | 1.68** |

* The lower and upper limits at the 95% confidence interval.
** The absolute lower and upper limits.

**Table 3. Statistics of the winter NAO index from 11 CMIP5 models. "Historical" refers to the period 1850-2005. "Future" refers to the period from 2050 to approximately the end of the 21st century, using the future scenario of RCP85.**

| *Model* | *Standard deviation of historical NAO index* | *Standard deviation of future NAO index* | *Change in mean future NAO index relative to past* |
|---|---|---|---|
| **CANESM2 ES** | 1.09 | 1.16 | -0.36 |
| **IPSL-CM5A-LR** | 1.19 | 1.18 | -0.14 |
| **IPSL-CM5A-MR** | 1.27 | 1.50 | 0.25 |
| **HADGEM2-ES** | 0.97 | 0.94 | -0.02 |
| **CNRM-CM5** | 1.08 | 1.08 | 0.00 |
| **GISS-E2-R** | 0.80 | 0.88 | 0.19 |
| **INMCM4** | 0.96 | 0.91 | -0.11 |
| **MRI-CGCM3** | 0.92 | 1.44 | -0.79 |
| **NORESM1** | 1.12 | 1.16 | 0.29 |
| **MPI-ESM-LR** | 1.13 | 1.07 | 0.35 |
| **CCSM4** | 1.07 | 1.05 | 0.35 |
| **Mean** | 1.05 | 1.12 | 0.00 |